

Action Spectroscopy and Photodissociation of Vibrationally Excited Methanol[†]

J. Matthew Hutchison,[‡] Robert J. Holiday, Andreas Bach,[§] Shizuka Hsieh,[#] and F. Fleming Crim*

Department of Chemistry, University of Wisconsin-Madison, Madison, Wisconsin 53706

Received: March 1, 2004; In Final Form: May 19, 2004

Vibrationally mediated photodissociation combined with time-of-flight detection of product H-atoms provides an electronic excitation action spectrum of jet-cooled methanol containing one quantum of O–H stretching excitation. The maximum in the electronic excitation spectrum of vibrationally excited methanol is about 2600 cm⁻¹ lower in total excitation energy than that for ground vibrational state methanol. A simple model using a one-dimensional vibrational wave function mapped onto a dissociative excited electronic state surface recovers the qualitative features of the spectrum. Using ab initio calculations of portions of the ground and excited potential energy surfaces, we calculate vibrational wave functions and simulate the electronic excitation spectra using the overlap integral for the bound and dissociative vibrational wave functions on the two surfaces. The qualitative agreement of the calculation with the measurement suggests that at the energy of the fundamental vibration the O–H stretch is largely uncoupled from the rest of the molecule during the dissociation.

I. Introduction

The broad and structureless ultraviolet absorption spectrum of methanol indicates that the first electronically excited state (S₁) of methanol dissociates rapidly.¹ The first absorption band is a 3s ← n transition to a Rydberg state that resembles the first electronically excited singlet state of water.^{2,3} Both bonds to oxygen are repulsive in the excited state since the 3s Rydberg character in the valence state correlates with σ* character in the exit channel.⁴ Extensive theoretical^{5–13} and experimental^{14–17} studies of dissociation of the prototypical water molecule show that vertical excitation places the system at the barrier between the exit channels, leading to equal probability of cleaving either O–H bond. The situation is only slightly more complicated in HOD where the mass difference in the two fragments leads to a 4-fold propensity for cleaving the O–H bond rather than the O–D bond.¹⁸ It is possible to alter the propensity for breaking the O–H bond by initially preparing HOD with an excited O–H stretching overtone vibration, an effect that comes from movement of the point of optimal overlap of the nuclear wave functions in the ground electronic state and the dissociative excited state out along the coordinate along the O–H coordinate. The vibrational excitation moves the point of maximum Franck–Condon overlap into one channel and, thus, biases the excited state dissociation.⁹ This selectivity disappears when the total excitation energy is large enough for the system to sample regions on both sides of the barrier that separates the two channels on the excited state surface.

The superficial similarities between methanol (CH₃OH) and partially deuterated water (HOD) raise the possibility that vibrational excitation could have a similarly dramatic effect on

the photodissociation of methanol. Satyapal et al.¹⁹ showed that dissociation to CH₃O and H is the dominant fate of methanol following excitation to the first excited singlet state (S₁ ← S₀) with 193-nm light. The quantum yield for these products is $\varphi = 0.86 \pm 0.10$, and about 82% of the available energy appears as relative translation of the products. The angular distribution of the hydrogen atoms is highly anisotropic, with an anisotropy parameter of $\beta = -0.60 \pm 0.03$, indicating that the lifetime of methanol in the S₁ state is shorter than its rotational period.¹⁹ Even though the S₁ surface is dissociative along the C–O coordinate, Satyapal, et al. find no evidence of the CH₃ + OH dissociation products.

Theoretical calculations explain many qualitative features of the one-photon photodissociation dynamics of methanol. Marston et al. calculated the energies of the ground S₀ and excited S₁ states²⁰ and mapped out portions of the surfaces by varying the O–H and C–O bond lengths, fixing the C–O–H angle and treating the methyl group as a “united atom”. Because the Franck–Condon region lies in the O–H dissociation channel of the S₁ surface, methanol molecules excited vertically from near their equilibrium geometry feel a strong gradient in the potential and rapidly dissociate to form CH₃O + H in preference to forming CH₃ + OH. Propagating wave packets on S₁ starting near the Franck–Condon point leads exclusively to CH₃O + H dissociation products with the CH₃ + OH channel opening only at much higher energies. In analogy with the observations and calculations for HOD, the calculations find that dissociating methanol containing at least five quanta of excitation in the C–O stretch does lead to the alternative products.²⁰

As a first step toward testing the influence of initial vibrational excitation, we have photodissociated methanol molecules initially prepared with one quantum of O–H stretching excitation. These vibrationally mediated photodissociation experiments prepare the system in a different region of the electronically excited state than is accessed in a one-photon dissociation. We have obtained the ground state vibrational action spectrum of the O–H stretch and an electronic action spectrum (S₁ ← S₀) of vibrationally excited methanol molecules prepared in a

[†] Part of the special issue “Richard Bersohn Memorial Issue”.

* Corresponding author. E-mail: fcrim@chem.wisc.edu.

[‡] Present address: Department of Chemistry and Biochemistry, Swarthmore College, Swarthmore, PA 19081.

[§] Present address: Laboratorium für Organische Chemie der ETH Zürich, CH-8093 Zürich, Switzerland.

[#] Present address: Department of Chemistry, Smith College, Northampton, MA 01063.

supersonic expansion. The electronic excitation occurs at a significantly lower total energy than is required to reach the electronically excited state in a one-photon excitation, which we simulate with a simple, one-dimensional model that essentially projects the ground state vibrational wave function onto the dissociative excited state potential energy surface.²¹

II. Experimental Approach

The experimental apparatus is a modified version of one used in other vibrationally mediated photodissociation experiments.^{22–24} Helium gas at a pressure of about 2000 Torr passes through a cell containing liquid methanol at 0 °C to form a mixture of ~1% methanol that passes through the 0.4-mm orifice of a pulsed valve to form a molecular beam that infrared excitation, ultraviolet photolysis, and ultraviolet probe laser beams intersect. Difference frequency generation in a 30-mm long LiNbO₃ crystal generates infrared light by mixing 1.064- μm light from an injection seeded Nd:YAG laser with that from a dye laser. Typical infrared pulse energies are 0.5–1 mJ in a bandwidth as small as $\Delta\tilde{\nu} = 0.05 \text{ cm}^{-1}$ at 3 μm . For reasons discussed below, we usually operate the laser without injection seeding in order to increase the infrared bandwidth to about 0.1 cm^{-1} . Frequency tripling the light from a second dye laser in two β -barium borate (BBO) crystals generates photolysis light in the range of 200–230 nm. We frequency double light from a third dye laser pumped by the second harmonic of a Nd:YAG laser to create ultraviolet 243-nm probe light for 2 + 1 REMPI detection of hydrogen atoms. The infrared light arrives 20 ns before the photolysis and probe lasers at a point in the expansion controlled by a digital delay generator. Two different lenses ($f = 150 \text{ mm}$ and $f = 350 \text{ mm}$, respectively) focus the counter propagating ultraviolet and infrared laser beams into the interaction region of a Wiley–McLaren time-of-flight mass spectrometer,²⁵ where they intersect the skimmed molecular beam.

The infrared light (λ_{vib}) excites the O–H stretch fundamental around 3680 cm^{-1} . The photolysis laser (λ_{phot}) promotes the vibrationally excited molecules to the S_1 surface, and a probe laser (λ_{probe}) ionizes the hydrogen atoms, which strike micro-channel plates at the end of the time-of-flight mass spectrometer. To correct for background photolysis of ground state methanol, we subtract the signal with the vibrational excitation laser blocked from the signal arising from all three lasers. (The background is about 10% at the maximum of the three-laser signal and is larger for other wavelengths.) Vibrational and electronic action spectra come from measuring the hydrogen ion signal due to the vibrational excitation laser while scanning the wavelengths of the vibrational excitation and photolysis lasers, respectively.

III. Results

The ability to dissociate vibrationally excited molecules preferentially allows us to obtain the vibrational action spectrum in the O–H stretching fundamental for methanol molecules cooled in the molecular beam. The top portion of Figure 1 is the photoacoustic spectrum of room temperature methanol. The transitions shown in gray are from small amounts of water in the photoacoustic cell and allow us to calibrate the wavelength of our infrared light using the HITRAN database.²⁶ The shape and width of the room temperature spectrum resembles the earlier low-resolution spectrum.²⁷ The lower portion of the figure is the vibrational action spectrum for methanol cooled by the expansion. The narrow envelope of rotational transitions reflects the substantial cooling, but we cannot extract a precise rotational

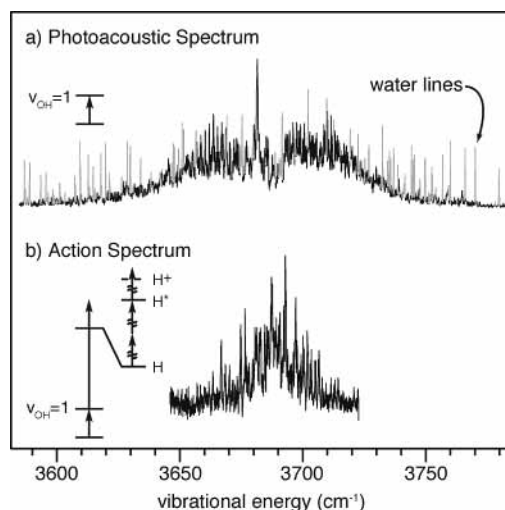


Figure 1. (a) Photoacoustic spectrum of the OH stretch fundamental band of methanol. Grey lines are due to residual water in the photoacoustic cell and serve to calibrate the vibrational wavenumber. (b) Action spectrum in the same spectral region of methanol cooled in the molecular beam. The spectral width indicates a rotational temperature of ~20 K.

temperature from the spectrum. Simulating the rotational–vibrational O–H stretch band using a symmetric top energy function and including asymmetry and torsional splittings^{28,29} does not recover the complex structure of the room temperature photoacoustic spectrum. However, we can estimate a rotational temperature of about 20 K by comparing the widths of the vibrational action spectrum with low-temperature simulations even though they do not reproduce all of the transitions.

There are several high-resolution studies exciting individual transitions in the O–H fundamental region of methanol,^{30–32} but because even our best infrared bandwidth (0.05 cm^{-1}) does not resolve all of the features in the spectrum, we generally do not prepare a single rotational level of the excited OH stretch. The exact torsional–rotational state we prepare is not an essential aspect of the subsequent excitation to the dissociative S_1 surface. Consequently, we use broader pulses from the unseeded laser to produce infrared light with a bandwidth of approximately 0.1 cm^{-1} to excite a range of rotational states and improve our signal-to-noise ratio.

Preparing methanol in the molecular beam with a quantum of O–H stretch by infrared excitation at 3693 cm^{-1} and scanning the wavelength of the photolysis laser provides the electronic excitation action spectrum for only the vibrationally excited molecules, shown as solid points in the upper panel of Figure 2. The plot shows the H-atom signal, normalized to the power of the ultraviolet photolysis light, as a function of the total energy added by the ultraviolet and infrared photons together. The open circles in the lower panel are the background signal from photolysis of molecules without initial vibrational excitation, and the solid line in the lower panel is the ultraviolet absorption spectrum¹ scaled to match the background signal at low energies. The maximum in the electronic excitation action spectrum of the vibrationally excited molecules is about 2600 cm^{-1} lower in energy than that for ground vibrational state molecules, reflecting the consequences of initial vibrational excitation. Clearly, initial vibrational excitation does more than simply increase the total energy available. The intensity of the spectrum for vibrationally excited molecules decreases sharply at $54\,000 \text{ cm}^{-1}$ where the one-photon excitation is most efficient. The large background from one-photon photolysis makes

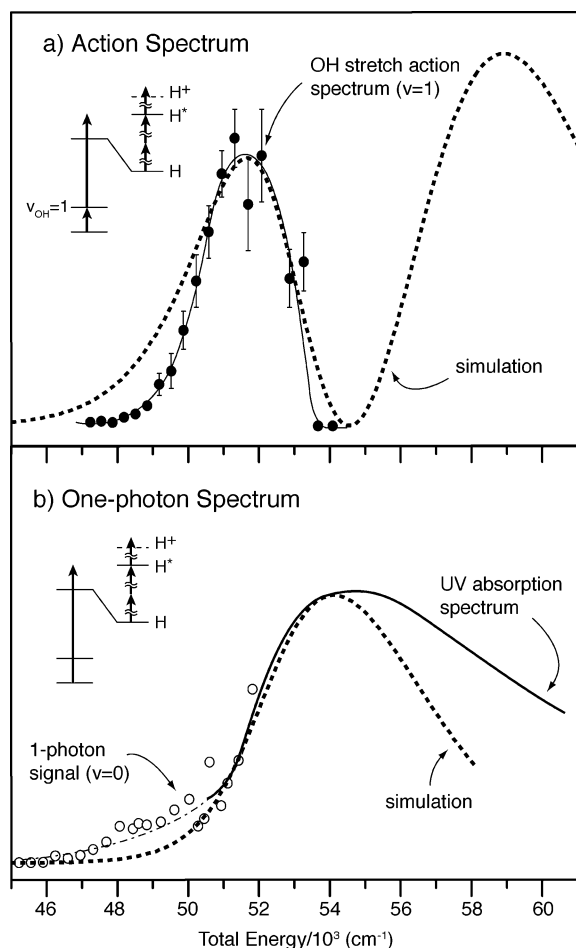


Figure 2. (a) Electronic action spectra of vibrationally excited ($\nu_{\text{OH}} = 1$) methanol. Filled circles indicate hydrogen ion signal due to both vibrational excitation and photolysis laser beams. The solid line through these data is a spline fit to help guide the eye. The simulation of the electronic excitation spectrum for the vibrationally excited molecules is shown with a dashed line. (b) One-photon absorption spectrum of ground state methanol. Open circles are signal due solely to the photolysis laser. The dash-dotted line is a spline fit through the open circles, which overlaps with the UV absorption spectrum (solid line) of Nee et al. (ref 1). The dashed line is the simulation of the absorption spectrum for ground state molecules.

detection of the vibrationally mediated process impossible at higher energies.

IV. Discussion

Excitation to a dissociative electronic state produces unstructured spectra. Because the dissociative state couples to a continuum, the simplest Franck–Condon picture of electronic absorption depends on the shape of the ground state vibrational wave function and total energy.³³ Vibrations perpendicular to the dissociation coordinate, the O–H stretch in the case of $\text{CH}_3\text{-OH}$, can complicate this simple picture. However, it is always the case that a vibrationally excited molecule samples a larger distribution of bond lengths and, hence, a larger range of excitation energies, than a ground vibrational state molecule, as illustrated by the one-dimensional potential energy curves (heavy lines) in Figure 3. The light curves in Figure 3 are the wave functions for the first two O–H stretching vibration levels in the ground electronic state and the dissociative wave function in the electronically excited state. Because the two potential curves are closer together at the outer turning point than at the equilibrium bond length, electronic excitation of a vibrationally

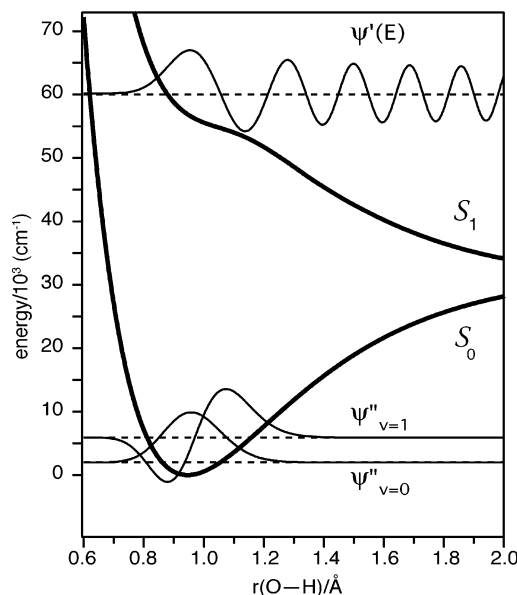


Figure 3. Cuts through the S_0 (lower) and S_1 (upper) potential energy surfaces in the OH coordinate of methanol calculated with CASSCF-(8,5)/6-31+G(d) (thick solid lines). Vibrational wave functions calculated from these potential surfaces are shown for the $\nu = 0$ and $\nu = 1$ states in S_0 and one dissociative wave function on S_1 (thin solid lines) at the energies indicated with dashed lines.

excited molecule can occur at a substantially lower energy than for a molecule closer to the equilibrium geometry. The substantial shift of the transition to lower total energy shown in Figure 2 is consistent with excitation from an excited vibrational state whose wave function extends further along the dissociation coordinate, as illustrated in the rudimentary one-dimensional model of Figure 3.

Even in the simplest picture, modeling the photodissociation at a single energy requires that we calculate the overlap integral involving the ground state vibrational wave function ψ''_v and a dissociative nuclear wave function ψ' on the excited state. In the one-dimensional model, the intensity of an electronic transition at frequency ν is proportional to³³

$$\nu \left| \int \psi'(E) \psi''_v dx \right|^2 \quad (1)$$

where E is the total energy above the dissociation asymptote. We generate one-dimensional potentials by calculating energies of both the S_0 and S_1 states using Gaussian³⁴ with the CASSCF-(8,5) method and a 6-31+G(d) basis set for O–H bond distances from 0.6 to 2.0 Å in 0.05 Å steps with the other degrees of freedom fixed at their equilibrium values. Test calculations at several points showed that relaxation of these degrees of freedom did not significantly alter the shape of the one-dimensional cuts shown in Figure 3. We use the Numerov method³⁵ to generate the one-dimensional vibrational wave functions for both potential surfaces and normalize the dissociative wave function using Child's procedure for continuum wave functions.³⁶ We ensure that the continuum wave functions at different energies E have the proper amplitudes relative to each other by using energy normalization, adjusting the calculated wave function to have a maximum amplitude of unity and dividing by $E^{1/4}$.³⁷ The wave functions shown as light curves in Figure 3 come from this calculation.

We simulate the electronic excitation spectra shown in Figure 2 as dashed lines for $\nu = 0$ and $\nu = 1$ of the O–H stretch by calculating intensities from eq 1 at a series of total excitation energies that include the zero-point energy in the ground state.

The calculated absorption for $\nu = 1$ begins at substantially lower energies than that for $\nu = 0$ with the calculated shift of 2400 cm^{-1} agreeing well with the experimental shift of 2600 cm^{-1} , most easily seen at the maxima. The total energy for both transitions is greater than the experimental excitation energy by 1400 cm^{-1} . This difference probably comes from the ab initio calculation of the S_1 energies, and we reduced the S_1 energies by 1400 cm^{-1} to bring the two into agreement. The adjusted one-dimensional calculation reproduces the maxima of the electronic excitation spectrum from both $\nu = 0$ and $\nu = 1$ and also mirrors the sharp decrease in the $\nu = 1$ electronic excitation spectrum at about 54 000 cm^{-1} .

It is striking that a simple one-dimensional model recovers the measured electronic absorption profile of vibrationally excited methanol so well. The calculation suggests that the sharp decrease in the spectrum for $\nu = 1$ near 54 000 cm^{-1} reflects the nodal structure of the vibrationally excited wave function in the ground electronic state and is consistent with initial excitation along the direction of the dissociation. Extensive coupling of the O–H stretch in the region of one quantum of excitation to other modes, either bound or unbound on the S_1 surface, would complicate the absorption profile of Figure 2.²¹ The success of our simple model suggests that the $\nu = 1$ level of the O–H stretch is not strongly coupled to other vibrational modes in either the ground or excited electronic state. This lack of coupling is the same behavior that Marston et al.²⁰ found in their calculations exploring coupling to the C–O bond. In addition, our test calculations on the S_0 and S_1 surfaces that allowed relaxation of all vibrational degrees of freedom showed no differences from the curves shown in Figure 2. This lack of coupling near the fundamental does not imply that higher levels of the O–H stretch are similarly isolated, and indeed, Rizzo and co-workers have demonstrated that such coupling is extensive for higher levels.^{38–44} Our measurements do not explore couplings among modes due to a lack of sensitivity in the electronic excitation spectrum. The most important conclusion is that the primary role of vibrational excitation of the fundamental O–H stretch in methanol is to allow the system to explore larger O–H bond distances than are accessible in the ground vibrational state to produce the attendant change in the electronic transition frequencies, which a rudimentary one-dimensional picture explains.

Acknowledgment. The authors thank the Division of Chemical Sciences of the Office of Basic Energy Sciences of the Department of Energy for the support of this work. We also thank Professors E. L. Sibert, T. R. Rizzo, and R. Schinke for extremely useful discussions on the spectroscopy and photodissociation of methanol.

References and Notes

- Nee, J. B.; Suto, M.; Lee, L. C. *Chem. Phys.* **1985**, *98*, 147.
- Robin, M. B. *Higher Excited States of Polyatomic Molecules*; Academic Press: New York, 1974; Vol. 1.
- Robin, M. B.; Kuebler, N. A. *J. Electron Spectrosc. Relat. Phenom.* **1972**, *1*, 13.
- Wen, Y.; Segall, J.; Dulligan, M.; Wittig, C. *J. Chem. Phys.* **1994**, *101*, 5665.
- Engel, V.; Schinke, R. *J. Chem. Phys.* **1988**, *88*, 6831.
- Engel, V.; Schinke, R.; Staemmler, V. *J. Chem. Phys.* **1988**, *88*, 129.
- Engel, V.; Staemmler, V.; Vander Wal, R. L.; Crim, F. F.; Sension, R. J.; Hudson, B.; Andresen, P.; Hennig, S.; Weide, K.; Schinke, R. *J. Phys. Chem.* **1992**, *96*, 3201.
- Schinke, R.; Vander Wal, R. L.; Scott, J. L.; Crim, F. F. *J. Chem. Phys.* **1991**, *94*, 283.
- Vander Wal, R. L.; Scott, J. L.; Crim, F. F.; Weide, K.; Schinke, R. *J. Chem. Phys.* **1991**, *94*, 3548.
- Imre, D. G.; Zhang, J. *Chem. Phys.* **1989**, *139*, 89.
- Zhang, J.; Imre, D. G. *J. Chem. Phys.* **1989**, *90*, 1666.
- Zhang, J.; Imre, D. G. *Chem. Phys. Lett.* **1988**, *149*, 233.
- Zhang, J.; Imre, D. G.; Frederick, J. H. *J. Phys. Chem.* **1989**, *93*, 1840.
- Vander Wal, R. L.; Scott, J. L.; Crim, F. F. *J. Chem. Phys.* **1991**, *94*, 1859.
- Vander Wal, R. L.; Scott, J. L.; Crim, F. F. *J. Chem. Phys.* **1990**, *92*, 803.
- Bar, I.; Cohen, Y.; David, D.; Arusi-Parpar, T.; Rosenwaks, S.; Valentini, J. J. *J. Chem. Phys.* **1991**, *95*, 3341.
- Bar, I.; Cohen, Y.; David, D.; Rosenwaks, S.; Valentini, J. J. *J. Chem. Phys.* **1990**, *93*, 2146.
- Shafer, N.; Satyapal, S.; Bersohn, R. *J. Chem. Phys.* **1989**, *90*, 6807.
- Satyapal, S.; Park, J.; Bersohn, R.; Katz, B. *J. Chem. Phys.* **1989**, *91*, 6873.
- Marston, C. C.; Weide, K.; Schinke, R.; Suter, H. U. *J. Chem. Phys.* **1993**, *98*, 4718.
- Schinke, R. *Photodissociation Dynamics: Spectroscopy and Fragmentation of Small Polyatomic Molecules*; Cambridge University Press: Cambridge, U.K.; New York, 1993.
- Bach, A.; Hutchison, J. M.; Holiday, R. J.; Crim, F. F. *J. Chem. Phys.* **2002**, *116*, 9315.
- Bach, A.; Hutchison, J. M.; Holiday, R. J.; Crim, F. F. *J. Phys. Chem. A* **2003**, *107*, 10490.
- Penn, S. M.; Hayden, C. C.; Muyskens, K. J. C.; Crim, F. F. *J. Chem. Phys.* **1988**, *89*, 2909.
- Wiley, W. C.; McLaren, I. H. *Rev. Sci. Instrum.* **1955**, *26*, 1150.
- Rothman, L. S.; Gamache, R. R.; Goldman, A.; Brown, L. R.; Toth, R. A.; Pickett, H. M.; Poynter, R. L.; Flaud, J. M.; Camy-Peyret, C.; et al. *Appl. Opt.* **1987**, *26*, 4058.
- Serrallach, A.; Meyer, R.; Gunthard, H. H. *J. Mol. Spectrosc.* **1974**, *52*, 94.
- Herzberg, G. *Molecular Spectra and Molecular Structure: II. Infrared and Raman Spectra of Polyatomic Molecules*; Van Nostrand Reinhold Co.: New York, 1945.
- Coudert, L.; Valentin, A. *J. Mol. Spectrosc.* **1987**, *122*, 390.
- Kleiner, I.; Fraser, G. T.; Hougen, J. T.; Pine, A. S. *J. Mol. Spectrosc.* **1991**, *147*, 155.
- Lee, R. G.; Hunt, R. H.; Plyler, E. K.; Dennison, D. M. *J. Mol. Spectrosc.* **1975**, *57*, 138.
- Carrick, P.; Curl, R. F.; Dawes, M.; Koester, E.; Murray, K. K.; Petri, M.; Richnow, M. L. *J. Mol. Struct.* **1990**, *223*, 171.
- Herzberg, G. *Molecular Spectra and Molecular Structure: I. Diatomic Molecules*; Prentice-Hall: New York, 1939.
- Frisch, M. J.; Trucks, G. W.; Schlegel, H. B.; Scuseria, G. E.; Robb, M. A.; Cheeseman, J. R.; Zakrzewski, V. G.; Montgomery, J. A.; Stratmann, R. E.; Burant, J. C.; Dapprich, S.; Millam, J. M.; Daniels, A. D.; Kudin, K. N.; Strain, M. C.; Farkas, O.; Tomasi, J.; Barone, V.; Cossi, M.; Cammi, R.; Mennucci, B.; Pomelli, C.; Adamo, C.; Clifford, S.; Ochterski, J.; Petersson, G. A.; Ayala, P. Y.; Cui, Q.; Morokuma, K.; Malick, D. K.; Rabuck, A. D.; Raghavachari, K.; Foresman, J. B.; Cioslowski, J.; Ortiz, J. V.; Baboul, A. G.; Stefanov, B. B.; Liu, G.; Liashenko, A.; Piskorz, P.; Komaromi, I.; Gomperts, R.; Martin, R. L.; Fox, D. J.; Keith, T.; Al-Laham, M. A.; Peng, C. Y.; Nanayakkara, A.; Gonzalez, C.; Challacombe, M.; Gill, P. M. W.; Johnson, B. G.; Chen, W.; Wong, M. W.; Andres, J. L.; Head-Gordon, M.; Replogle, E. S.; Pople, J. A. *Gaussian 98*, revision A.7; Gaussian, Inc.: Pittsburgh, PA, 1998.
- Levine, I. N. *Quantum Chemistry*, 4th ed.; Allyn and Bacon: Boston, 1991.
- Child, M. S. *Molecular Collision Theory*; Academic Press: London; New York, 1974.
- Sibert, E. L. Personal communication.
- Boyarkin, O. V.; Lubich, L.; Settle, R. D. F.; Perry, D. S.; Rizzo, T. R. *J. Chem. Phys.* **1997**, *107*, 8409.
- Lubich, L.; Boyarkin, O. V.; Settle, R. D. F.; Perry, D. S.; Rizzo, T. R. *Faraday Discuss.* **1995**, *102*, 167.
- Chirokolava, A.; Perry, D. S.; Boyarkin, O. V.; Schmid, M.; Rizzo, T. R. *J. Mol. Spectrosc.* **2002**, *211*, 221.
- Boyarkin, O. V.; Rizzo, T. R.; Perry, D. S. *J. Chem. Phys.* **1999**, *110*, 11359.
- Boyarkin, O. V.; Rizzo, T. R.; Perry, D. S. *J. Chem. Phys.* **1999**, *110*, 11346.
- Chirokolava, A.; Perry, D. S.; Boyarkin, O. V.; Schmid, M.; Rizzo, T. R. *J. Chem. Phys.* **2000**, *113*, 10068.
- Rueda, D.; Boyarkin, O. V.; Rizzo, T. R.; Mukhopadhyay, I.; Perry, D. S. *J. Chem. Phys.* **2002**, *116*, 91.